International Conference on Applied Energy 2020
Nov 29 – Dec 02, 2020, Bangkok, Thailand
Paper ID: 372

COMPARISON OF DIFFERENT MODELS OF THERMOELECTRIC GENERATORS AND OPTIMIZATION OF THEIR GEOMETRIC STRUCTURES

Wei He, Guangsen Yao, Zihan Cai, Jifang Zhang, Ying Shi, Kai Zhu

Tianjin Key Laboratory of Refrigeration Technology, Tianjin University of Commerce, Tianjin 300134, PR China

ABSTRACT

A three-dimensional numerical model of a thermoelectric module (TEM) is constructed using COMSOL simulation software basing on HZ-type thermoelectric material. First, the different models are compared with considering variable physical property and equal internal resistance or not. Then, the geometric structure on P(N) leg of TEM is optimized by taking the power density as the optimal objective. The results show that the optimal geometric size combination of p-n legs is l_{opt} = 6.9 mm and h_{opt} = 0.8 mm. The peak power density with optimal structure can increase by 75% compared to Hz products.

Keywords: thermoelectric generator, model, geometric size

1. INTRODUCTION

The use of waste heat to generate electricity has become an important research topic [1]. Compared with traditional power generation technology, this technology has the outstanding advantages of no pollution, no noise, no moving parts, and high reliability [2].

In recent years, the performance index of thermoelectric materials has significantly improved [3]. However, optimization of the module structure based on high-performance thermoelectric materials is still an effective way to improve the thermoelectric performance of thermoelectric generator (TEG) [4]. From the aspect of high-efficiency thermoelectric module design, there have many published articles related to thermoelectric unit groups and thermal module numerical models, such as Jang et al. [5], which established a micro-TEG composed of a single p-n pair. The effects of the thickness of the ceramic plate and the cross-sectional area of the leg on output power and efficiency were studied using a constant-physical-property calculation method with a small temperature difference of 15 °C. Rezania et al. [6] focus on the single p-n pair, and the ratio of cross-sectional area between P-type and N-type legs is optimized. In terms of TEG structure optimization, the present optimization mainly focused on the leg geometry for a micro-TEG composed of a single p-n pair mostly, and took maximum output power as the optimal objective. In this paper, the P(N) leg optimization is done based on multiple p-n pairs and different models where the power density is taken as the optimal objective. Moreover, the influence of different working temperature on the optimal p-n leg size is explored.

2. THERMOELECTRIC MODEL

2.1 Model formulation

In this study, COMSOL Multiphysics software is used to construct a numerical model of a three-dimensional thermoelectric generator. Fig. 1 illustrates a small TEM model composed of multiple p-n pairs. The P(N) legs are connected in series by a copper connector and are placed between two ceramic pieces. Referring to current TEM product, the model assumes that the P-leg and N-leg have the same size, and the length and width of the P(N) legs are always the same, described by *l* (side

length). Parameters *h* represent the height of the P(N) legs.

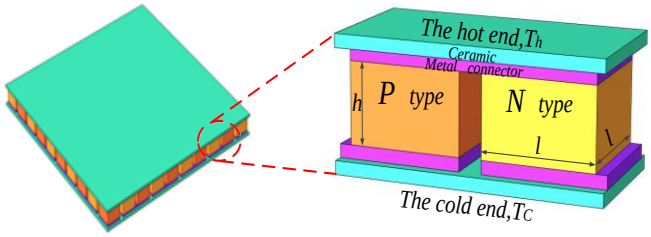

Fig 1 Schematic of thermoelectric generator module

In the model calculation, the cold and hot end temperatures are taken as T_c and T_h, respectively, in this paper, the fixed cold end temperature is 50°C. The thermoelectric material properties in the model are derived from the HZ product parameters [7], as shown in Table 1. The working conditions are steady, the contact resistance generated by solder is not considered, there is no air inside the TEM, and all thermal radiation is neglected. All other surfaces contacting with the outside are set as thermal insulation and electrical insulation surfaces. The contact thermal resistance between the ceramic plate, copper and P(N) legs is taken as 0.0001 $m^2 K W^{-1}$ [8]. The load resistance R_{load} is connected outside the generator to form a loop. One end of the module connected to the generator is grounded; that is, the potential V = 0. The thermoelectric coupling differential equation describes the current density J and heat flux JQ as follows:

$$\begin{aligned} -\mathbf{J} &= \sigma\nabla V + \sigma\alpha\nabla T \\ \mathbf{J}_Q &= -\kappa\nabla T + T\alpha\mathbf{J} \end{aligned} \tag{1}$$

Here, σ is the conductivity, V is the potential, α is the Seebeck coefficient, T is the temperature, and κ is the thermal conductivity. In the $\boldsymbol{J}$ equation, the first term equal to $\boldsymbol{J}$ represents the Ohm's law, and the second term is the Seebeck effect. In the $\boldsymbol{J}_Q$ equation, the first term is the Fourier heat conduction, and the second term is the Peltier effect.

In steady-state operation, the current density does not diverge,

$$\nabla\cdot\mathbf{J} = 0, \tag{2}$$

while for heat flux,

$$\nabla\cdot\mathbf{J}_Q = -\nabla\cdot(V\mathbf{J}). \tag{3}$$

For steady-state operation, the energy accumulation must be zero,

$$\dot{e} = \nabla\cdot(\kappa\nabla T) - \nabla\cdot((V+T\alpha)\mathbf{J}) = 0. \tag{4}$$

Since the current is non-divergent, the energy accumulation becomes

$$\dot{e} = \nabla\cdot(\kappa\nabla T) - \mathbf{J}\cdot(\sigma^{-1}\mathbf{J}) - T\nabla\alpha\cdot\mathbf{J} \tag{5}$$

where the middle term is Joule heating and the latter is the Thomson effect, both of which are included in the simulation.

According to the Seebeck effect, the electromotive force produced by the generator can be represented by

$$E = \alpha\left(T_h - T_c\right). \tag{6}$$

For the current generated in the circuit,

$$I = \frac{E}{R_{in} + R_{load}} \tag{7}$$

and

$$R_{in} = \frac{\left(1/\sigma_P + 1/\sigma_N\right)h}{a^2} \times N \tag{8}$$

where R_{in} is the internal resistance of the generator, N is the number of p-n pairs.

Therefore, the expression of generator output power is

$$P_{out} = I^2 R_{load}, \tag{9}$$

while the power density is given by

$$P_{pers} = P_{out} / A \tag{10}$$

where A is the total area of the generator module.

Table 1 Physical-property parameters of HZ thermoelectric material

Parameter	*Value*
α_P(V/K)	$1.1134 \times 10^{-14}T^4 - 2.035\times10^{-11}T^3 + 1.113344\times10^{-8}T^2 - 1.818175\times10^{-6}T + 1.61\times10^{-4}$
σ_p(S/m)	$1/\ (-4.32 \times 10^{-16}T^4 + 8.9397 \times 10^{-13}T^3 - 7.74 \times 10^{-10}T^2 + 3.519405 \times 10^{-7}T - 5.01 \times 10^{-5})$
κ_p(W/(m·K))	$-1.242 \times 10^{-9}T^4 + 2.3307 \times 10^{-6}T^3 - 1.57451 \times 10^{-3}T^2 + 4.5698175 \times 10^{-1}T - 46.97059$
α_N(V/K)	$-1.3 \times 10^{-14}T^4 + 2.3254 \times 10^{-11}T^3 - 1.4202 \times 10^{-8}T^2 + 3.4691 \times 10^{-6}T - 4.4276 \times 10^{-4}$
σ_N(S/m)	$1/\ (1.317 \times 10^{-16}T^4 - 2.305 \times 10^{-13}T^3 + 7.8272 \times 10^{-11}T^2 + 4.5066 \times 10^{-8}T - 8.072 \times 10^{-6})$
κ_N(W/(m·K))	$1.5365 \times 10^{-10}T^4 - 3.019 \times 10^{-7}T^3 + 2.2458 \times 10^{-4}T^2 + 7.414466 \times 10^{-2}T + 10.124244$

2.2 *Model validation*

To verify the reliability of the mathematical model. Ensuring that the size and physical parameters of the model are exactly the same as the provided product HZ-14, and the simulation data are compared with the product HZ-14 data by using the variable-physical-property calculation method, the output power under different load resistances is calculated. Fig. 2 shows the comparison results of the product value and simulation value. The figure shows that the data of the two groups of output power have a high degree of coincidence, with a maximum relative error of 8.8%. The deviation is within the acceptable range, which verifies the accuracy of the

model.

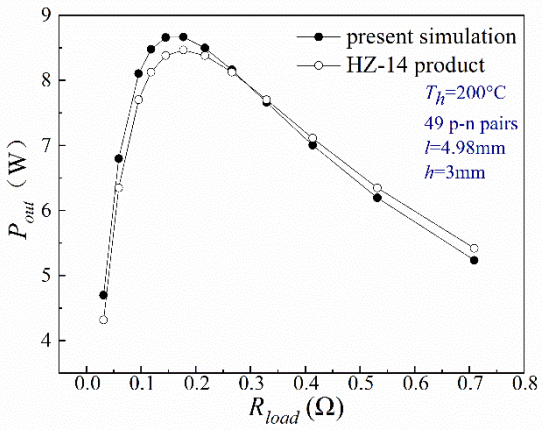

Fig 2 Present numerical model validation by comparison with product data

3. RESULTS AND DISCUSSION

3.1 Comparison of different TEM models

In order to simplify the calculation, a single p-n pair TEM is adopted here. Generally, a constant physical property of TE material is taken in TEM. However, the TE material actions a variable physical property with temperature changes actually. Therefore, the thermoelectric performance is compared between constant physical property case and variable physical property case. Fig. 3 shows the mutative rule of the output power with load resistance under the two cases of variable and constant properties. As shown in the Fig.3, the output power contains a certain error under the calculation of variable and constant physical properties. The maximum output power P_{1max}, P_{2max} can be obtained at their corresponding optimal load resistance values R_{1opt}, R_{2opt}. To compare the relative errors of the maximum output power and optimal load resistance of constant properties relative to variable properties, the following power deviation (DP_1) and resistance deviation (DR_1) are introduced by $DP_1=\left|P_{2\max}-P_{1\max}\right|/P_{1\max}\times100$ and $DR_1=\left|R_{2opt}-R_{1opt}\right|/R_{1opt}\times100$. For the case as shown in Fig.3, there is DP_1=0.96%, DR_1=2.86%.

Generally, it is assumed that the load resistance is equal to the internal resistance in normal constant physical thermoelectric model. However, for the case shown in Fig.3, the optimal load resistance shows obviously deviation from the internal resistance for the constant physical case, P_{Rin} is the value at corresponding internal resistance value R_{in} as shown in Fig. 3. To compare the relative errors of the output power and load resistance of optimal resistance case relative to equal internal resistance case, the power deviation (DP_2) and resistance deviation (DR_2) are introduced by $DP_2=\left|P_{in}-P_{1\max}\right|/P_{1\max}\times100$ and $DR_2=\left|R_{in}-R_{1opt}\right|/R_{1opt}\times100$.

For the case as shown in Fig.3, there is DP_2=1.04%, DR_2=22.86%.

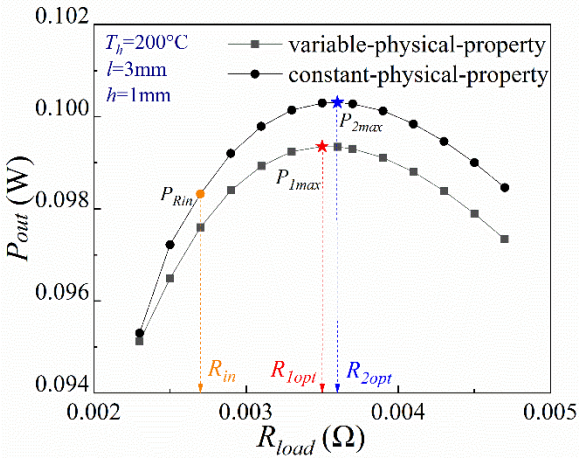

Fig. 3 Power output for different load resistance

To explore the influence of different leg geometry sizes on the relative error, based on the conventional design of leg size, a side length range of 1–11 mm and height range of 1–5 mm is considered, and the corresponding power deviation (DP_1, DP_2) and resistance deviation (DR_1, DR_2)are calculated. Fig. 4 and 5 show the deviation values for different geometric dimensions. Fig. 4 shows that the leg geometric sizes have an obvious influence on both DR_1 and DR_2, and the highest resistance deviation (marked by DR_{1max} and DR_{2max}) can reach to about (11% and 31%), respectively. Fig. 5 shows that DP_1 varies less with side length but increases with leg height, with maximum deviation (marked by DP_{1max}) at a side length of 3 mm. The influence of geometry size on DP_2 presents an unstable rule, which includes the comprehensive influence of multiple factors, such as geometry, physical property, and load matching. The maximum DP_2 (marked by DP_{2max}) exits at a side length of 11 mm. However, DP_{1max} and DP_{2max} are both less than 3%.

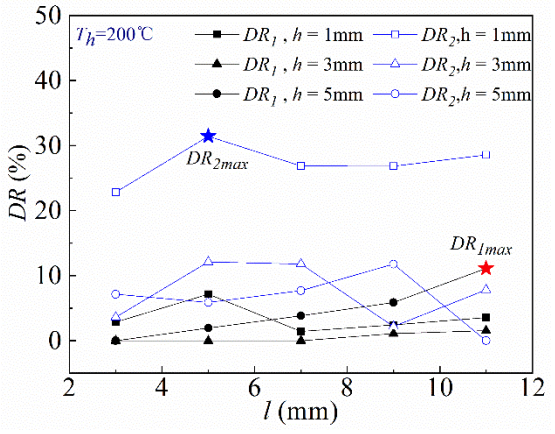

Fig. 4 Relative error of resistance under different geometric sizes

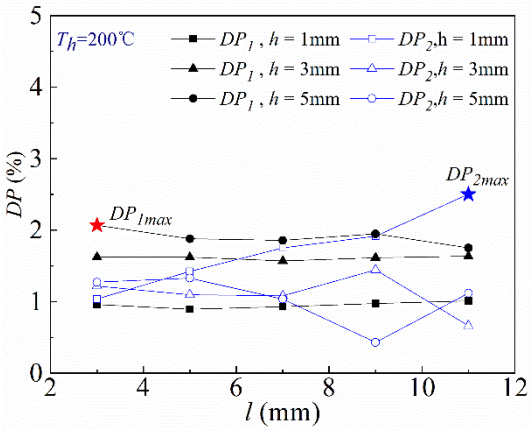

Fig. 5 Relative error of output power under different geometric sizes

To further determine the influence of operating temperature on the maximum power deviation (DP_{1max} and DP_{2max}) and resistance deviation (DR_{1max} and DR_{2max}), Fig. 6 shows the maximum deviation values within the conventional size range of the leg at different hot-end temperatures. From it, the four parameters all fluctuate within different temperature ranges; however, they are all controlled within a certain range. In summary, within the conventional geometric size range and applicable operating temperature range, the final maximum values of DP_{1max}, DP_{2max}, DR_{1max}, and DR_{2max} are 8.5%, 8.2%, 11.1%, and 31.4%, respectively.

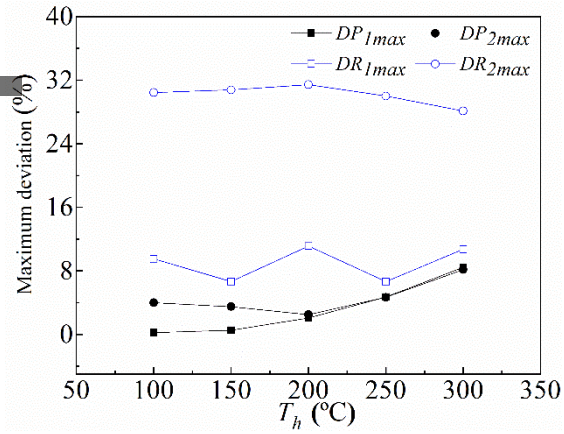

Fig. 6 Relative error for different hot-end temperatures

3.2 *Geometric Size Optimization of the TEM*

For a better fit in practical application, the geometric size optimization of the small generator module composed of 50 p-n pairs will have greater practical significance. Next, the common model, which takes constant physical parameters and equal load resistance assumption is adopted in the geometric size optimization. In this example of the TEM model, the maximum power density is taken as the optimization goal.

First, the leg side length (l) is optimized as shown in Fig. 7. From it, the output power keeps increasing as the leg side length increases, but there is an optimal leg side length (l_{opt}) for which the power density value is the highest. For the different heights, the optimal side length and its corresponding maximum power density value are shown in Fig. 8. From it, l_{opt} increases with increasing height but the maximum power density increases at first and then decrease with increasing height. Therefore, there is an optimal height (h_{opt}) and corresponding optimal side length combination that maximizes the power density value (marked as P_{peak} in figure 8).

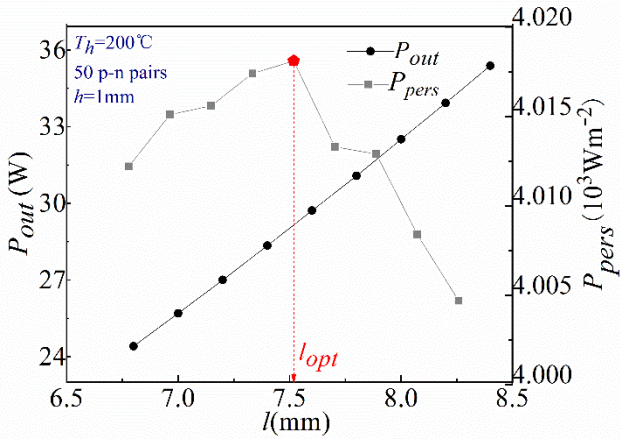

Fig. 7 Output power and power density for different side lengths

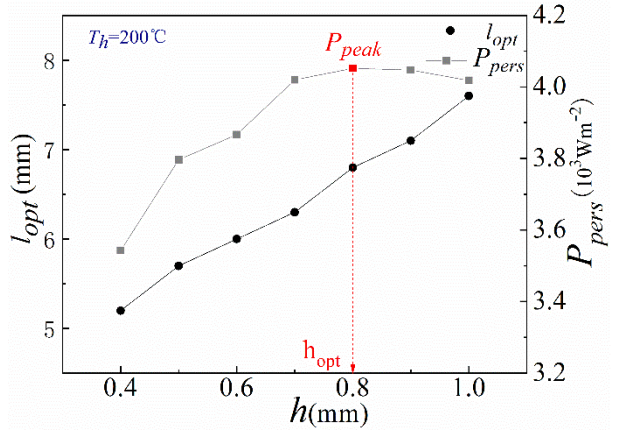

Fig. 8 Optimal side length and power density for different heights

Fig.9 shows the corresponding peak power density, optimal leg side length and height under various hot-end temperatures. It can be seen that, with an increase in the hot-end temperature, the peak power density increases significantly, optimal width increases slowly, and optimal height decreases slowly. Compared with HZ-14 products, the peak power density is greatly increased with optimal

structure, and the biggest increase of peak power density rate is 75% at T_h=300°C.

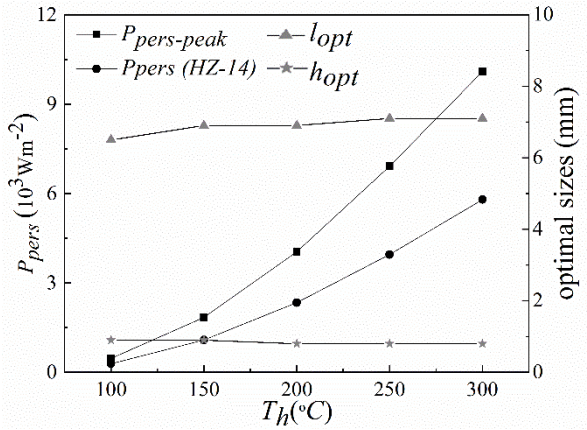

Fig. 9 Optimal state value for different hot-end temperatures

4. CONCLUSION

In the range of T_h ∈ (100-300℃), T_C = 50℃, a TEM with equal leg side length is established for HZ thermoelectric materials. The error of the combination model of constant physical property and equal internal resistance is explored, and the geometric size of the leg is optimized. The results are as follows:

(1) Although the maximum error of the internal resistance relative to the optimal load is 31.4%, When the optimal load with constant physical properties and the equal internal resistance with constant physical properties are adopted, the maximum errors of output power are 8.5% and 8.2% respectively, for the conventional geometric size and working temperature range. Therefore, constant physical properties and the equal internal resistance can simplify the calculation significantly and yield a small relative error.

(2) There is an optimal height h_{opt} and corresponding optimal side length l_{opt} combination that maximizes the power density. The l_{opt} = 7.3 mm and h_{opt} = 0.8 mm can be used as the reference for the values of the optimal geometric design, which is suitable for all operating temperatures in the normal range for HZ material.

(3) The peak power density increases significantly with an increase in the hot-end temperature. The optimization on P(N) leg sizes can significantly improve the output performance of TEM. The peak power density with optimal structure can increase by 75% compared to Hz-14 products.

ACKNOWLEDGEMENTS

The authors are grateful for the financial support from the National Fundamental Research Program of China (51806152), the International Cooperation Research Program of MOST (2017YFE0198000), and the International Clean Energy Talent Program by China Scholarship Council.

REFERENCE

[1] Negash A A, Kim T Y, Cho G. Effect of electrical array configuration of thermoelectric modules on waste heat recovery of thermoelectric generator. J Sensors & Actuators A Physical, 2017; S0924424717306283.

[2] He W, Wang S, Lu C, et al. Influence of different cooling methods on thermoelectric performance of an engine exhaust gas waste heat recovery system[J]. Applied Energy, 2015; 162(1):1251-1258.

[3] Alam H, Ramakrishna S. A review on the enhancement of figure of merit from bulk to nano-thermoelectric materials. J Nano Energy, 2013; 2(2):190-212.

[4] Alberto Ferrario, Stefano Boldrini, Alvise Miozzo. Temperature dependent iterative model of thermoelectric generator including thermal losses in passive elements. J Applied Thermal Engineering, 2019; 150: 620-627

[5] Jang B, Han S, Kim J Y. Optimal design for micro-thermoelectric generators using finite element analysis. J Microelectronic Engineering, 2011： 88:775-778.

[6] Rezania A. Parametric optimization of thermoelectric elements footprint for maximum power generation. J Power Sources, 2014;255:151–6.

[7] web: www.Hi-z.com.

[8] Hailong He, Yi Wu, Weiwei Liu. Comprehensive modeling for geometric optimization of a thermoelectric generator module. J Energy Conversion and Management,2019;183: 645-659